Proc. 16th Intern Workshop on Rare-Earth Magnets and Their Applications, Sendai, Japan, Sept. 10-13, 2000.

BNL-67257

Effect of Pre-Alloying Condition on the Bulk Amorphous Alloy $Nd_{60}Fe_{30}Al_{10}$

A. S. O'Connor[*], L. H. Lewis[**], R. W. McCallum[*], K. W. Dennis[*], M. J. Kramer[*], D. T. Kim Anh[***], N. H. Dan[****], N. H. Luong[***], and N. X. Phuc[****]

[*]*Ames Laboratory and Department of Materials Science and Engineering, Iowa State University, Ames, Iowa 50011 U.S.A.*

[**]*Materials and Chemical Sciences Division, Department of Applied Science, Brookhaven National Laboratory, Upton, New York 11973-5000 U.S.A.*

[***]*Center for Materials Science, Hanoi National University, 90 Nguyen Trai, Dong Da, Hanoi, VIETNAM.*

[****]*National Center for Science and Technology, Institute of Materials Science, Hoang Q. Viet Street, Hanoi, VIETNAM.*

Abstract

Bulk metallic glasses are materials that require only modest cooling rates to obtain amorphous solids directly from the melt. $Nd_{60}Fe_{30}Al_{10}$ has been reported to be a ferromagnetic bulk metallic glass that exhibits high coercivity, a combination unlike conventional Nd-based amorphous magnetic alloys. To clarify the relationship between short-range order and high coercivity in glassy $Nd_{60}Fe_{30}Al_{10}$, experiments were performed to verify the existence of a homogeneous liquid state prior to rapid solidification. Alloys were prepared by various pre-alloying routes and then melt-spun. Arc-melted alloys were prepared for melt spinning using three different protocols involving: 1) alloying all three elements at once, 2) forming a Nd-Fe alloy which was subsequently alloyed with Al, and 3) forming a Fe-Al alloy for subsequent alloying with Nd. XRD, DTA, and magnetic measurement data from the resultant ribbons indicate significant differences in both the glassy fraction and the crystalline phase present in the as-spun material. These observed differences are attributed to the presence of highly stable nanoscopic aluminide- and/or silicide-phases, or motes, present in the melt prior to solidification. These motes would affect the short-range order and coercivity of the resultant glassy state and are anticipated to provide heterogeneous nucleation sites for crystallization.

Introduction

Bulk metallic glasses constitute a unique family of metal alloys that requires only a modest cooling rate, 1-100 K/s, to form an amorphous solid from the melt. The lack of long-range order and grain boundaries in bulk metallic glass alloys enables them to exhibit superplasticity and enhanced corrosion resistance, conferring great technological potential. Recent reports[1] claim that $Nd_{60}Fe_{30}Al_{10}$ is a ferromagnetic bulk metallic glass that is amorphous and yet exhibits a high magnetic coercivity, on the order of 277 kA/m. This behavior is in contradiction to that found in well-understood conventional Nd-based amorphous magnetic alloys.[2] In conventional alloys, especially $Nd_2Fe_{14}B$, an amorphous microstructure yields soft magnetic characteristics with negligible coercivity.[3] Coercivity does not develop in the $Nd_2Fe_{14}B$ alloys unless the material

contains a significant fraction of the crystalline phase, easily detected by x-ray diffraction (XRD). The high coercivity arises from impediments to domain wall motion, caused by grain boundaries or other defects. The origin of impediments to domain wall motion is unclear in bulk amorphous magnetic alloys with high coercivities. One hypothesis is that clusters of differing local composition with disparate magnetic properties exist in the bulk amorphous alloy and confer coercivity. To clarify the relationship between potential existence of short-range order and coercivity in these alloys, investigations of the glass formability, magnetic character, and thermal stability were made in a series of melt-spun ribbons based on the composition $Nd_{60}Fe_{30}Al_{10}$. It is expected that the solidification route, microstructure, and composition of melt-spun ribbons of this composition are more homogeneous than those of their bulk analog. Understanding obtained from studies on melt-spun ribbons will later be applied to studies on bulk cast forms of the material.

Procedure

The composition chosen for investigation was based on published experiments to identify the best glass-forming composition in the Nd-Fe-Al system.[4] Samples of the composition $Nd_{60}Fe_{30}Al_{10}$ were made using three different routes. Three different pre-alloyed starting charges were prepared by arc-melting the constituent high-purity elements under an atmosphere of 0.7 bar high purity Ar in different sequences: Fe and Al were combined and Nd alloyed in later, Nd and Fe were combined and Al added later, and all three elements were pre-alloyed simultaneously. These three pre-alloying conditions are referred to as (Fe,Al)+Nd, (Nd,Fe)+Al, and (Nd,Fe,Al), respectively. Each arc-melted sample was subsequently induction melted in a quartz crucible to 1000°C and then melt-spun on a copper wheel spinning with a tangential surface speed of 25 m/s, in 1/3 atmosphere of helium.[5] The side of the resultant melt-spun ribbon in contact with the wheel is the “wheel side," while the other side of the ribbon is the “free side.” XRD, differential thermal analysis (DTA), and magnetic measurements were performed on each sample. The XRD was performed on both ground ribbon samples and on the free side of melt-spun ribbons using a Philips diffractometer and Cu-K_α radiation. The DTA on each sample was performed from room temperature to 1000°C at a heating rate of 20°C per minute in Ar flowing at 100 cc/min using a Perkin Elmer DTA7. For DTA, the ribbon pieces were placed in an Al_2O_3 crucible and covered with dehydrated MgO powder to enhance thermal contact and to minimize reaction with the Al_2O_3 crucible, which produced a strong exothermic reaction with the melt-spun ribbons immediately following melting. Magnetic measurements were performed with a Quantum Design MPMS SQUID magnetometer at T=300 K from 5 Tesla (4 MA/m) to -5 Tesla (-4 MA/m), using multiple ribbon pieces measured parallel to the applied field.

Results

Data derived from XRD, DTA, and magnetic measurements indicate that the resultant melt-spun ribbons exhibit significant differences in microstructure and phase constitution.

I. XRD

The differences between the XRD patterns in Figures 1 and 2 indicate that pre-alloying order does affect the phases present in the melt-spun ribbons. XRD patterns for ground ribbons (Fig. 1) show minor differences among the microstructures of the ribbons produced from the three different pre-alloyed conditions. Both the samples of (Fe,Al)+Nd and (Nd,Fe)+Al have some long-rang crystallographic order as evidenced by low-intensity broad peaks that occur in an amorphous background. The (Nd,Fe,Al) pattern appears to be almost completely amorphous.

The XRD patterns obtained from the free side of the melt-spun ribbons also show clear differences between the samples (Fig. 2). If nucleation from the melt occurs, the thermal gradient across the thickness of the ribbon during melt spinning is sufficient for grain growth, resulting in microstructural and phase differences through the thickness of the ribbon.[5] Therefore XRD of the free side surface of the ribbons is a more rigorous test for the presence of

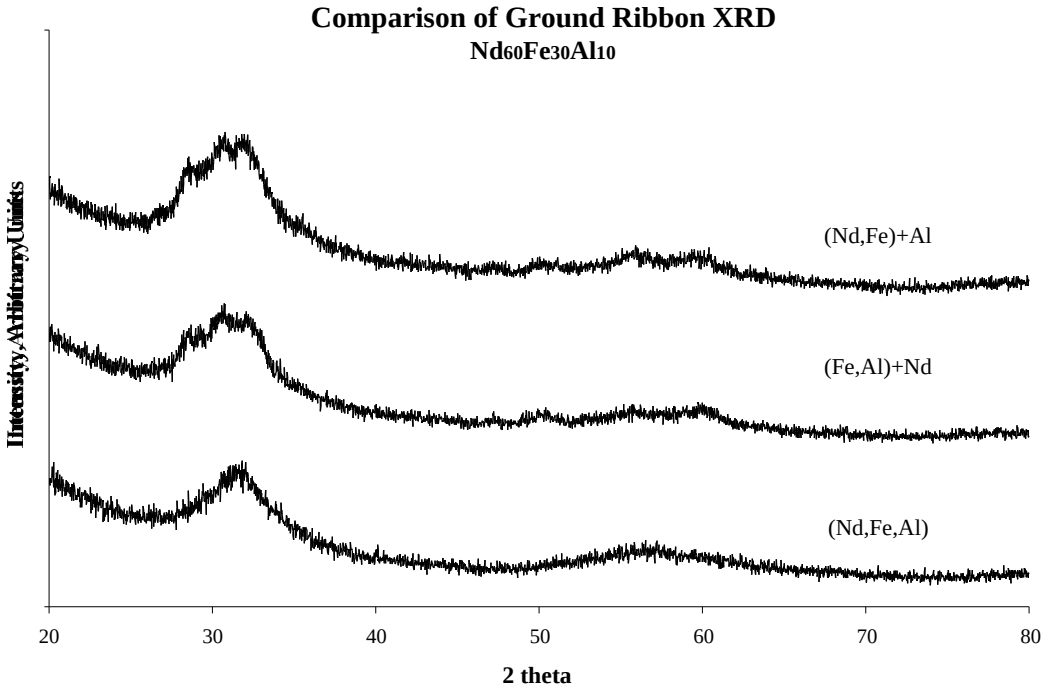

Figure 1: Comparison of effect of pre-alloying conditions on XRD patterns of the ground melt-spun ribbons for 3 different $Nd_{60}Fe_{30}Al_{10}$ pre-alloys.

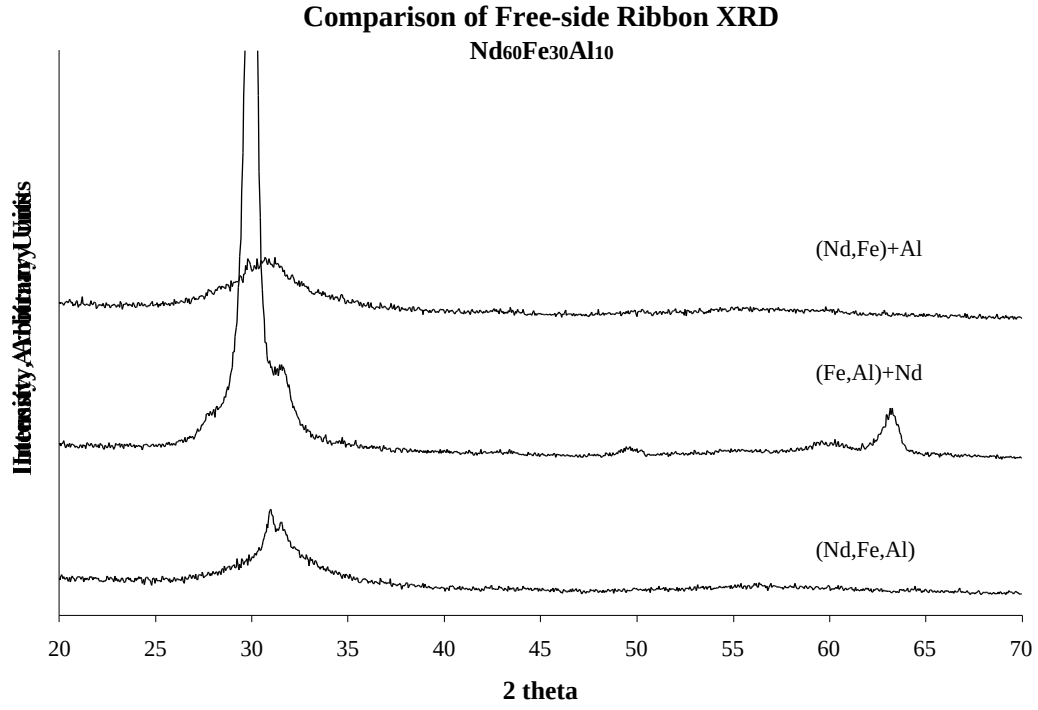

nucleated phases and better displays the intersample differences arising from the different pre-alloying conditions. All three samples have a broad amorphous-type peak located around 2Θ = 31º that indicates the sample is largely amorphous. The (Fe,Al)+Nd sample appears to have the largest crystalline fraction of the three samples, with a very strong peak centered at 2Θ = 30º, as well as several smaller, broad XRD peaks. The (Nd,Fe,Al) sample exhibits evidence of the presence of nanocrystalline material characterized by weak Bragg reflections centered near the amorphous peak. The (Nd,Fe)+Al sample exhibits no obvious crystalline Bragg peaks under our measurement conditions. The differences between Figures 1 and 2 can be explained if the nucleated phases apparent in Figure 2 are essentially near-surface features that represent a small fraction of the bulk of the material.

II. DTA

While all three samples show DTA exothermic signals with onset temperatures around 460°C, there are substantial differences in the character of the decompositions (Fig. 3).

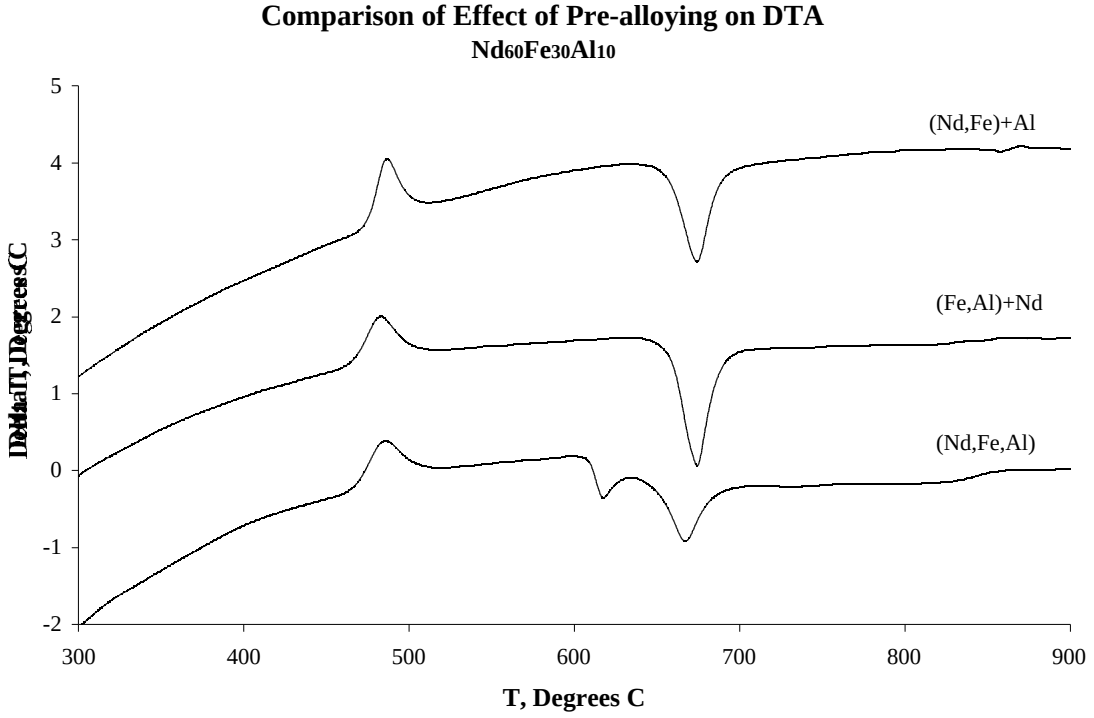

Figure 3: Comparison of effect of pre-alloying conditions on DTA performed on melt-spun ribbons for 3 different $Nd_{60}Fe_{30}Al_{10}$ pre-alloys.

The (Nd,Fe)+Al sample has the largest crystallization peak area. As the crystallization peak area is proportional to the crystallization energy times the volume fraction, the largest peak area should represent the largest fraction of amorphous material of the three samples (Table 1). The (Nd,Fe,Al) sample has the next largest crystallization peak area, and the (Fe,Al)+Nd sample has the smallest crystallization peak area. These results correspond closely to those obtained from

the XRD data. Both of the two-step pre-alloyed samples have very similar endothermic events, with onsets occurring between 657 and 659°C. The one-step pre-alloy sample, (Fe,Al,Nd), has two endothermic signals, one with an onset temperature at 610°C and the second with an onset temperature of 651°C. The single endotherms that occur near 660°C are attributed to crystallization of the glass to the known equilibrium phase composition.[6] The double endotherm in the (Nd,Fe,Al) sample is inconsistent with the equilibrium phase distribution at this composition. As there are no crystalline phases in the equilibrium phase diagram near the composition of the glass, the presence of a significant crystalline fraction must result in a change in the composition of the remaining glassy fraction. If the crystalline fraction identity does not correspond to the equilibrium phase for this composition, the composition of the glass may be shifted into a different phase field in the ternary equilibrium phase diagram and result in a different final phase assemblage or different reaction pathway for this composition. In all three samples a minor DTA anomaly at 845°C indicates the liquidus temperature, which is in reasonable agreement with the reported equilibrium value of near 800°C.[6]

III. Magnetization Measurements

The room temperature magnetization data also show significant differences in the samples of the three pre-alloying conditions (Fig. 4). The (Nd,Fe)+Al sample has the highest remanence and coercivity of the three samples, followed closely by (Fe,Al)+Nd and with (Nd,Fe,Al) having the smallest values. Typically, Nd-based amorphous magnetic alloys show soft magnetic characteristics, with little remanence or coercivity. None of the samples prepared here are particularly soft, but the low remanence and coercivity of the (Nd,Fe,Al) sample makes it the softest, and most likely most homogeneous, sample of the three. The magnetization values at high field also vary between the samples. The differences in the magnetic data can be accounted for by the presence of anti-ferromagnetic phases or ferromagnetic phases with ordering below room temperature present in different amounts in each of the samples.

Sample	**XRD Bragg peak** Appearance	**DTA** Crystallization Peak Area, J/g	**Magnetization** H_c, kA/m	M at 5T, kA/m	M_R, kA/m
(Nd,Fe)+Al	Broad peak at d=2.88	-23.3	25.1	16.97	3.41
(Fe,Al)+Nd	Stronger peaks at d=2.98, 2.83, 1.83, 1.55, 1.47	-20.1	21.6	15.61	2.70
(Nd,Fe,Al)	Sharpening of broad peak at d=2.88, 2.83	-21.7	3.49	13.50	0.84

Table 1: Summary of experimental findings.

IV. Discussion

From the differences observed in the XRD, DTA, and magnetic measurement data, it is clear that the phase composition of the melt-spun material is dependent on the order in which the constituents are alloyed. This conclusion can only be true if a homogeneous liquid state is not obtained prior to solidification. As each of the binary phase diagrams of these elements shows the presence of refractory phases, there is a distinct possibility that non-equilibrium refractory phases may be formed during the initial alloy preparation. These phases can be slow to dissolve into the melt during subsequent melting. By pre-alloying the constituent elements, i.e., by arc-

melting Nd and Fe then adding Al, or by arc-melting Fe and Al and then adding Nd, it is possible to control the reaction sequence and possibly avoid the formation of any refractory phases.

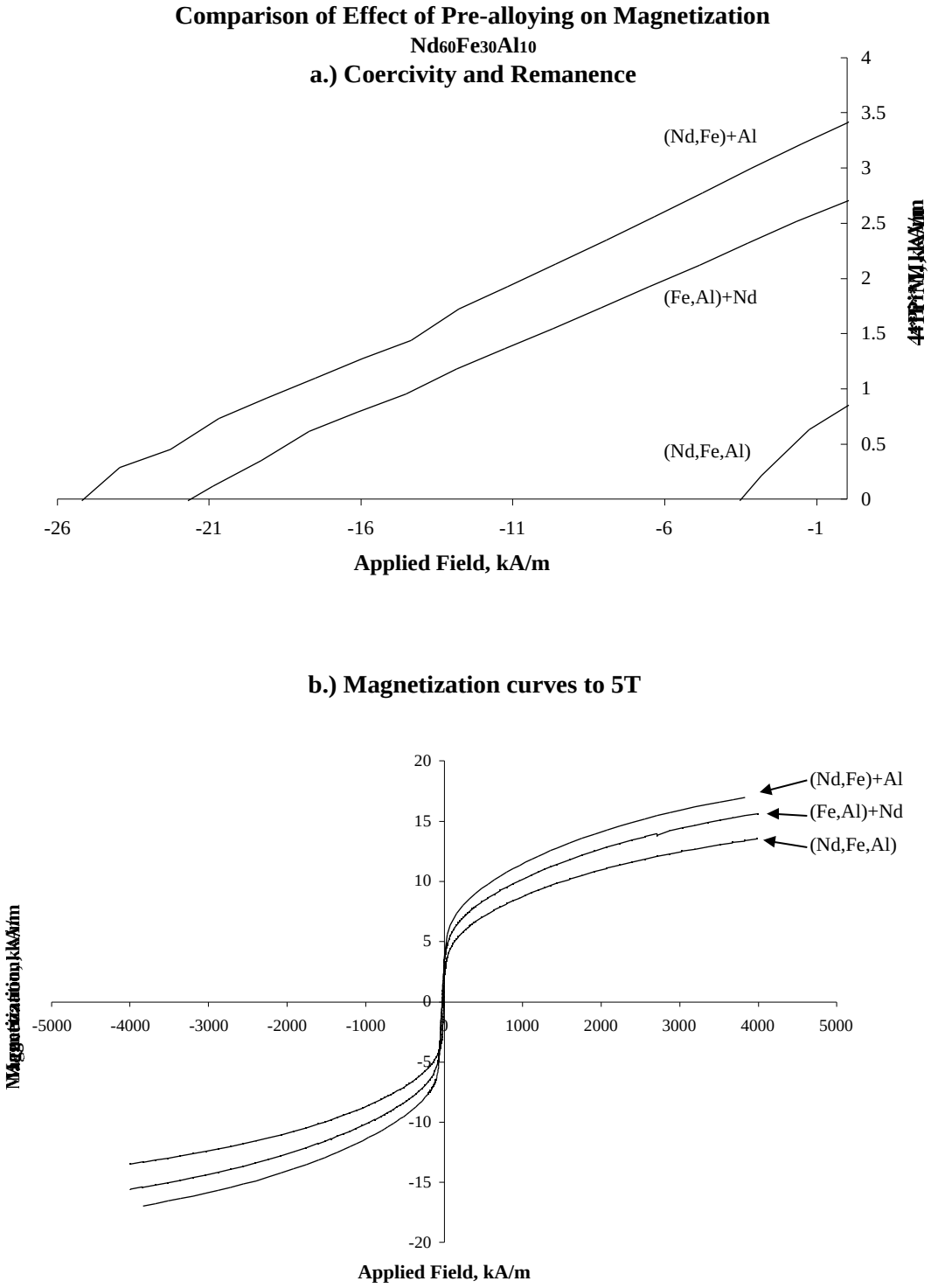

Figure 4: Effect of pre-alloying condition on magnetization measurement. a.) Magnified view of second-quadrant demagnetization curve showing remanence and coercivity. b.) Full magnetization curves to 5T (4 MA/m) applied field.

When the three elements are arc-melted together without any pre-alloying, as in (Nd,Fe,Al), the local conditions may be significantly different from those of the pre-alloyed case. Since Al is the lowest melting-point element of the three constituents, as the temperature is raised molten Al surrounds the solid Nd and Fe. Since diffusion in the liquid is much more rapid than diffusion in the solid, the phases formed between Nd and Al are approached from the Al-rich side during arc melting. Thus the initial conditions are favorable for the formation of $NdAl_2$, which, with a melting point of 1460°C, is the most refractory phase in the Nd-Al system. For arc-melted samples, the inability to produce homogeneous samples in systems which display wide variations in melting points is in no sense unique to Nd-Fe-Al but rather is a well known shortcoming of the technique. Even though the ratio of Nd and Al in $Nd_{60}Fe_{30}Al_{10}$ is near the Nd-Al eutectic, the superheat temperature attained during the induction melting prior to melt spinning may still be insufficient to homogenize the sample, and it is likely that some of the $NdAl_2$ would remain as nanoscopic motes in the melt, acting as nucleation sites.

In the Fe-Al binary pre-alloy charge, the Fe:Al composition should form the stable $\alpha-Fe$ phase for T > 855°C. This Fe:Al ratio in $Nd_{60}Fe_{30}Al_{10}$ is approached from the Al-rich side, where only lower-melting phases occur. These phases include $FeAl_3$ and Fe_2Al_5, with 1160ºC < T_{melt} < 1170ºC. Since the temperature reached during induction melting prior to melt spinning is below these temperatures, it is possible that these phases, if present, do not fully dissolve in the melt before solidification. For the Nd-Fe binary pre-alloyed charge, the phases formed are approached from the Nd-rich side. The Nd:Fe composition used for the pre-alloyed charges possesses a liquidus at about 820°C. The most probable crystalline phase formed at this Nd:Fe compositional ratio is the $Fe_{17}Nd_2$ phase, but it is less likely that any refractory phases form between Nd and Fe compared to the (Al,Nd,Fe) and (Al,Fe)+Nd binary pre-alloyed charges.

In all cases, the arc-melted samples are expected to be fully crystalline and multi-phase. The weight fraction of residual refractory phase should be well below the limit of detectability for x-ray diffraction and thus no attempt was made to identify the phases in the arc-melted buttons. While it seems likely that refractory binary phases would form in the pre-alloyed charges, there are no detectable binary phases present in the XRD data for the melt spun (Nd,Fe,Al) or the (Nd,Fe)+Al samples. Additionally, the strong peaks evident in the (Fe,Al)+Nd pattern do not correspond to any single Fe-Al binary compound diffraction pattern. However, there may be some correlation between these peaks and the presence of some aluminide phases or ternary phases. Additional phase analysis is underway.

Other sources for motes that may act as nucleation sites may be silicides. The quartz crucibles used to induction melt the alloys prior to melt spinning impart some silicon to the samples during induction melting. Inductively Couple Plasma Atomic Emission Spectroscopy, ICP-AES, has shown the level of Si incorporation varies with temperature. Although the contamination is low (< 2.5 at. %), the Si readily forms very refractory phases with Nd, Fe, and Al, any of which could provide nucleation sites for crystalline phases. However, the presence of these phases is not expected to be dependent on the alloying route.

The sub-solidus region of the ternary phase diagram at the composition $Nd_{60}Fe_{30}Al_{10}$ lies in a two-phase region between Nd and $Nd_6Fe_{13-x}Al_{1+x}$ ($0.6 < x < 4$). This condition suggests the

possibility of formation of nanoscopic clusters of locally varying composition, some hypothesized to be rich in Nd and others rich in Fe, relative to the average composition. The composition of these local nanoclusters would be influenced by any pre-existing crystallinity that forces the composition of the remaining glass out of the two-phase region. It is speculated that the presence of such ferromagnetic clusters could account for the differences in coercivity and remanence seen in the samples of this study.

Conclusions

From the data presented here, it can be seen that the pre-alloying sequence prior to melt spinning of the ferromagnetic bulk metallic glass composition $Nd_{60}Fe_{30}Al_{10}$ results in differing phase assemblages and microstructures. Pre-alloying Nd and Fe before adding Al results in a nearly-homogeneous amorphous alloy after melt spinning as determined by XRD and DTA. Pre-alloying of Fe and Al before adding Nd results in a mixture of crystalline and amorphous phases, while the fraction of glassy phase obtained from pre-alloying all three metals at once was intermediate to that of the other samples. It is concluded that differences in the microstructures and phase constitutions of the resultant melt-spun materials would only occur if a homogeneous liquid is not attained prior to melt spinning.

Acknowledgements

Research performed under the auspices of the U.S. Dept. of Energy, at Ames Laboratory under Contract No. W-7405-ENG-82 and the Division of Materials Sciences, Office of Basic Energy Sciences under contract No. DE-AC02-98CH10886 at Brookhaven National Laboratory. Support from the East Asia and Pacific Program of the Division of International Programs, the U.S. National Science Foundation, is gratefully acknowledged. We would also like to acknowledge Les Reed and Zack Meissen for their expertise in sample preparation and Susan Collins for experimental assistance.

References

[1]Akihisa Inoue, Tao Zhang, and Akira Takeuchi, *IEEE Trans. Magn.* **33** 3814 (1997).
[2]J. F. Herbst, *Rev. of Mod. Phys.* **63** n.4 819 (1991).
[3]Raja K. Mishra, *J. of Magnetism and Mag. Mat.* **54-57** 450 (1986).
[4]Akihisa Inoue, Akira Takeuchi, and Tao Zhang, *Met. and Mat. Trans. A* **29A** 1780 (1998).
[5]M. J. Kramer, Yali Tang, K. W. Dennis, and R. W. McCallum, *Mat. Res. Soc. Symp. Proc.* 577 57-62 (1999).
[6]Bernd Grieb and Ernst-Theo Henig, *Z. Metallkde* **82** 560 (1991).